Ann. Geophys., 32, 739–748, 2014
www.ann-geophys.net/32/739/2014/
doi:10.5194/angeo-32-739-2014

Annales Geophysicae
Open Access

First report of sporadic Na layers at Qingdao (36° N, 120° E), China

Z. Ma[1,2], X. Wang[1,2], L. Chen[1], and J. Wu[2]

[1]China Research Institute of Radiowave Propagation, Qingdao, Shandong, China
[2]National Key Laboratory of Electromagnetic Environment, Qingdao, Shandong, China

Correspondence to: Z. Ma (zh.zh.ma.7@gmail.com)

Received: 18 January 2014 – Revised: 25 May 2014 – Accepted: 27 May 2014 – Published: 2 July 2014

Abstract. This paper reports, for the first time, observational results of mesopause sporadic Na (Na_s) layers by a ground-based lidar at Qingdao (36° N, 120° E), China. Based on ∼430 h of observational data on 95 nights from December 2007 to June 2012, we have selected a total of 53 Na_s layer events. It is found that characteristics of Na_s layers over Qingdao have general similarity with those over nearby sites, Wuhan (30° N, 114° E) and Hefei (32° N, 117° E), but not those over the site Hachioji (35° N, 139° E) at nearly the same latitude as Qingdao. At the same time, parameters of sporadic E (E_s) layers were recorded by an ionosonde. The fact that E_s layer occurrence probabilities of 19, 22, and 18 % in time intervals before, during, and after the Na_s layers are very close to the average occurrence ratio of the nocturnal E_s layer (21 %), may reveal a general independence between Na_s and E_s layers over Qingdao. Only those strong Na_s layers above the peak altitude of the main Na layer might have a significant correlation with E_s layers. In addition, a total of 11 high-altitude (above 105 km) Na_s layer events have been surveyed specially. It is found that these high-altitude Na_s layers were usually weak. And they possessed long-duration (> 147 min) and broad-layer width (4.0 km) compared with Na_s layers below 105 km (> 96 min and 2.4 km). These characteristics are in accord with observational results at Wuhan. It is suggested that there is little correlation between this kind of Na_s layers and E_s layers. Finally, the summer topside enhancement phenomenon of Na atoms observed at Qingdao is in accord with several earlier observational results at different sites (18, 30, and 54° N) in the Northern Hemisphere.

Keywords. Atmospheric composition and structure (middle atmosphere – composition and chemistry)

1 Introduction

Free metal atoms are present in Earth's mesopause region between 75 and 110 km. Among Na, Fe, K, and Ca, Na is most widely observed. Lidar measurements indicate that the number density profile of Na atoms roughly possesses the Gaussian shape with height and peaks at ∼92 km normally. However, besides this normal layer (main layer), Na atoms can be sporadically enhanced within a narrow height range, which has been defined as a sporadic Na (Na_s) layer (Hansen and von Zahn, 1990; Clemesha et al., 1999).

The characteristics of Na_s layers have been widely surveyed. Despite the narrow height region (typically ∼2 km full width at half maximum, FWHM) of Na_s layers, they can exhibit horizontal sizes between 100 and 2000 km measured by multiple-point observations (Batista et al., 1991; Kane et al., 1991). The occurring altitude of Na_s layers is generally higher than the peak of the main layer and normally falls with time (Clemesha, 1995). The decay period of Na_s layers is normally longer than their formation period (Kwon et al., 1988; von Zahn et al., 1987). In addition, simultaneous and common volume lidar observations at 30° N showed that, 62 % of sporadic Na and Fe (Fe_s) layers occurred in overlapping altitude ranges and moved following almost the same track (Yi et al., 2007). Occasionally, Na_s layers could appear at extremely high altitude (above 105 km) (Collins et al., 1996; Yi et al., 2002; Gong et al., 2003; Ma and Yi, 2010; Dou et al., 2013). Through a statistics study, Ma and Yi (2010) have found that Na_s and Fe_s layers above 105 km at 30° N occurred mostly during summer and possessed long durations and broad layer widths.

However, the formation mechanism of Na_s layers is still not very clear. Through simultaneous observations of sporadic E, Na, Fe, and Ca ion layers at Urbana, Illinois, Gardner et al. (1993) suggested that high-altitude Na_s layers would

be formed by the neutralization of Na ion in an associated sporadic E (E_s) layer. A high correlation between the occurrences of Na_s layers and E_s layers has led to suggesting the neutralization of the Na ion reservoir in the E_s layers as a source of the neutral Na atoms (von Zahn and Hansen, 1988; Beatty et al., 1989; Kane and Gardner, 1993; Cox and Plane, 1998; Clemesha et al., 1999; Shibata et al., 2006; Williams et al., 2006, 2007; Delgado et al., 2012; Yuan et al., 2013; Dou et al., 2013). In addition, according to several chemical theoretical studies, the Na ion is converted into a Na atom at a height around or above 100 km (Cox and Plane, 1998; Hansen and von Zahn, 1990; Collins et al., 2002). Also, the observations indicated that, sporadic neutral atom (N_s) layers correlated with E_s layers were likely to appear around 100 km (Beatty et al., 1989; Friedman et al., 2000; Williams et al., 2007). Nevertheless, the correlation of N_s layers and E_s layers is not 1 : 1 (Clemesha, 1995). Observations at 69° N indicated that no E_s layer appeared within 2 h before and after the occurrence of some Na_s layers and Fe_s layers (Hansen and von Zahn, 1990; Alpers et al., 1994). Through the observations at different locations, Alpers et al. (1994) have found that the correlation between Fe_s and E_s layer events exhibited obvious latitudinal variation. Through statistics work, it was found that the probability of a Na_s layer simultaneously appearing with the E_s layer was low (32 %) at 69° N (Hansen and von Zahn, 1990). The geographical distribution characteristics of correlation between N_s and E_s layers are very obscure.

Another origin of Na_s layers may be direct meteoric injection, as source of metallic materials among the mesopause. The first report of a sporadic Na layer suggested that it resulted from meteor deposition (Clemesha et al., 1978). It has been suggested that the high-altitude sporadic metal layers might belong to a different population and have different origin (Hansen and von Zahn, 1990; Kane and Gardner, 1993; Clemesha, 1995). Höffner and Friedman (2004, 2005) suggested a direct link between ablating meteoroids and topside metal layers. Through a statistical study, Ma and Yi (2010) suggested the Northern Hemisphere high-altitude sporadic layers occurring mostly during summer would come from enhanced micro-meteoroid influx.

In this study we present observational results of Na_s layers obtained by ground-based lidar at 36° N, as well as the statistical results of correlation between Na_s and E_s layers. In addition, high-altitude Na_s layers are surveyed.

2 Instruments

The multifunctional aerosol-temperature-sodium (ATS) lidar of the China Research Institute of Radiowave Propagation (CRIRP) can detect the lower atmosphere and aerosols by Mie and Raman scattering, as well as the middle atmosphere by Rayleigh and Na resonance fluorescence scattering. It first came into operation in June 2006 at Qingdao (36° N, 120° E), China. Observations are performed routinely at night and one of the operational modes is adopted roughly alternately for each night. The lidar parameters related with Na resonance fluorescence detection are given in Table 1.

Table 1. Lidar parameters related to Na resonance fluorescence detection.

Transmitter		
Laser	Continuum 8020 Nd:YAG Laser	ND6000 DYE Laser
Wavelength	532 nm	589 nm
Linewidth	1 cm^{-1}	0.5 cm^{-1}
Pulse energy	550 mJ (typ.)	70 mJ (typ.)
Repetition rate	20 Hz	20 Hz
Pulse width	5–7 ns	5–7 ns
Beam expander	× 2.5	
Beam divergence (after beam expander)	0.3 mrad	0.6 mrad
Receiver		
Telescope aperture	Cassegrain 1 m	
Field of view	2 mrad	
Filter		
Bandwidth	0.5 nm	
Transmission ratio	60 %	

The time bin length is 1 µs corresponding to the range bin length of 150 m. The time resolution of Na profiles is normally 250 s (5000 laser shots), and was adjusted to 300 s (6000 laser shots) from 20 February to 15 October 2009. The pointing of the transmitting beam is established by scanning the backscatter signal at 30 km along two perpendicular directions. The pointing of the laser beam is established by the trapezoid method (Fiorani et al., 1998). The wavelength is tuned up by scanning the maximum backscatter signal strength of Na atom at 90 km. The Na atom number density is obtained by contrasting the resonance fluorescence scattering signal of Na atoms to the Rayleigh scattering signal of the atmosphere at 30 km.

The ionosonde of CRIRP is located at a horizontal distance of only ∼ 30 m away from the lidar. Its frequency sweeps from 1 to 32 MHz in ∼ 1 min, and the altitude uncertainty for sporadic E layers is ±5 km. This ionosonde operates every hour on the hour. Consequently, the data period of E_s layers cover all Na data. The ionograms are scaled according to the *Manual of Ionogram Scaling* by Wakai et al. (1987).

3 General overview of sporadic Na layers

Our observations of Na atoms by lidar were first performed in December 2007, and the data used in this study are up to June 2012. In order to ensure a good data quality, profiles with a threshold number density (the number density

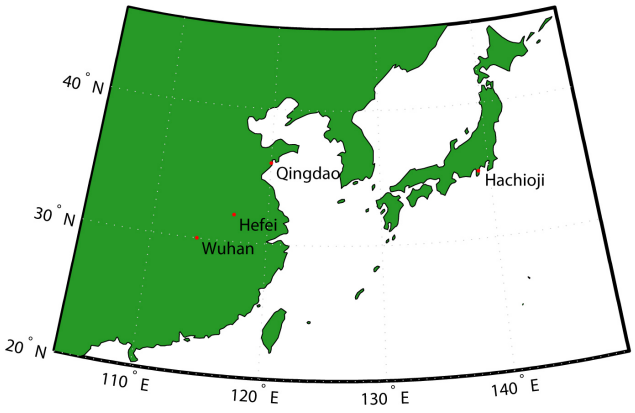

Figure 1. A map showing the relative positions of four lidar sites.

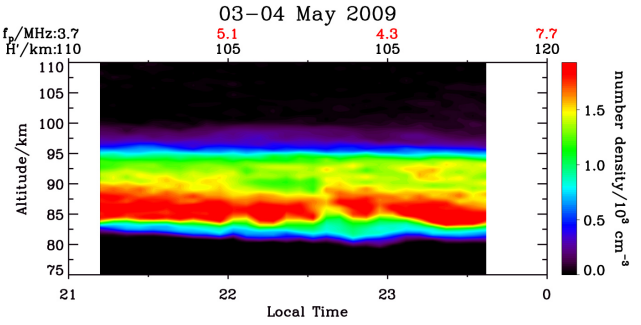

Figure 2. Na density contour plot and E_s layer parameters during the night of 3–4 May 2009. For detailed explanation please see text. Notice the E_s layer occurred without any Na_s layer during the entire observation of Na layers.

corresponding to one single photon in one range bin) above 40 cm^{-3} at 90 km have been excluded. Then we have obtained ∼ 430 h of Na number density data on 95 nights totally. Observation was performed at least three times in each month except in July.

To be classified as a sporadic layer, the peak Na density must be equal to or greater than twice that of the background Na density (Clemesha et al., 1999). In addition, the peak number density is required to reach 500 cm^{-3}, and a sporadic layer should last at least for three successive profiles. According to these criteria, a total of 53 sporadic Na layer events have been selected from ∼ 430 h of data.

Through a statistical study of all these sporadic Na layer events, we have obtained their characteristics exhibited in Table 2. For comparison, Table 2 also list characteristics of Na_s layers gained at another three lidar sites (Wuhan, Hefei, and Hachioji). Figure 1 is the map showing the relative positions of these four lidar sites. The distance between Wuhan/Hefei and Qingdao (∼ 900/500 km) is nearer than that between Hachioji and Qingdao (∼ 1700 km), whereas Hachioji (35° N) is nearly at the same latitude as Qingdao (36° N). As seen in Table 2, it is found that the occurrence rate and strength (average peak density, maximum peak density, average peak abundance and maximum peak abundance) of Na_s layers over Qingdao are all close to those over Wuhan. The average width and altitude of Na_s layers over Qingdao are close to those over Hefei. However, the strength (average peak density and maximum peak density) and average altitude of Na_s layers over Qingdao are much different with those over Hachioji. Overall, characteristics of Na_s layers over Qingdao have the general similarity with those over nearby sites, Wuhan and Hefei, but not with those over the site Hachioji, which is nearly at the same latitude as Qingdao. Thus the observations of Na_s layers over these four locations show little latitudinal dependence but are sensitive to longitude. Of course, we recognize that the data analysis and identification criteria of sporadic layers may have some difference for different observing locations.

In the next section, we will survey the temporal correlation between sporadic Na and E layers by both case and statistical studies. And we will further study the correlation between sporadic Na and E layers by surveying E_s layer occurrence probabilities in three different time intervals around Na_s layers in Sect. 5. Then Sect. 6 will pay attention to characteristics of high-altitude (above 105 km) sporadic Na layers.

4 Correlation between sporadic Na and E layers

The strength of a sporadic E layer detected by ionosonde is normally directly recorded by the plasma frequency, f_p (MHz), which is related to the electron concentration ($N_e = 1.24 \times 10^4 f_p^2$ cm^{-3}). First of all, a proper strength criterion (threshold f_p) for judging the E_s layer event should be established. Based on the nighttime (19:00–05:00 LT – local time) data by ionosonde from December 2007 to June 2012, the calculated probabilities for f_p reaching 3, 4, and 5 MHz are 29, 21, and 14 %, respectively. Thus we set the threshold f_p of E_s layers to 4 MHz (Dou et al., 2013), in order to ensure a similar ratio of event duration to total observation duration with Na_s layers (19 %, as seen in Table 2). Thus, a recognized E_s layer only represents one with f_p of or exceeding 4 MHz in the following.

4.1 Case studies

4.1.1 Case study 1 (3–4 May 2009)

Figure 2 shows the Na density contour plot and E_s layer parameters during the night on 3–4 May 2009. The color contour plot is the Na density with height and time. The two rows of values on the upper abscissa are plasma frequency (above) and virtual reflection height in kilometers, as recorded hourly by the ionosonde. The f_p in red color represents the occurrence of the E_s layer. We point out that the virtual height of an E_s layer will be slightly higher than its actual height due to the slowing of radiowave propagation in

Table 2. Statistical characteristics of Na_s layers observed at different lidar sites in the midlatitude region.

Parameters	Na_s layers			
Location	Wuhan	Hefei	Hachioji	Qingdao
Latitude and longitude	30° N, 114° E	32° N, 117° E	35° N, 139° E	36° N, 120° E
Distance from Qingdao/km	∼ 900	∼ 500	∼ 1700	0
Reference	Yi et al. (2007)	Dou et al. (2009)	Nagasawa and Abo (1995)	this work
Number of observed Na_s layer	30	64	> 100	53
Occurrence rate/h^{-1}	1/6.5	1/14	1/10	1/8.1
Ratio of event duration to total observation duration	35 %	NA	20 %	19 %
Average formation period/min	72	> 56	NA	> 48
Average duration/h	> 2.3	> 2.25	> 2.0	> 1.6
Average peak density/cm^{-3}	7270	6170	<2870	7510
Maximum peak density/cm^{-3}	41 760	17 380	8800	34 560
Average peak abundance/cm^{-2}	1.1×10^9	NA	NA	1.4×10^9
Maximum peak abundance/cm^{-2}	4.2×10^9	NA	NA	4.8×10^9
Average width (FWHM)/km	2.1	2.6	NA	2.4
Average altitude of maximum density/km	96.1	94.8	97.8	94.4

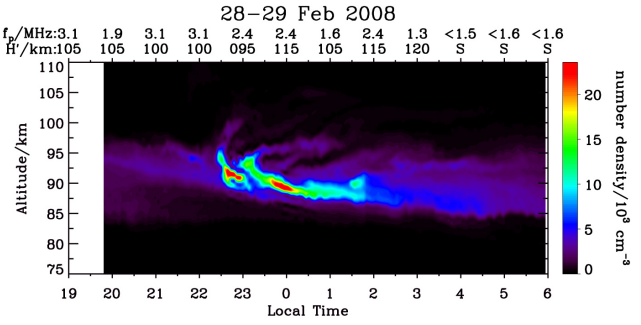

Figure 3. Na density contour plot and E_s layer parameters during the night of 28–29 February 2008. Note an extremely strong Na_s layer burst around 22:39 LT without any E_s layer throughout the night.

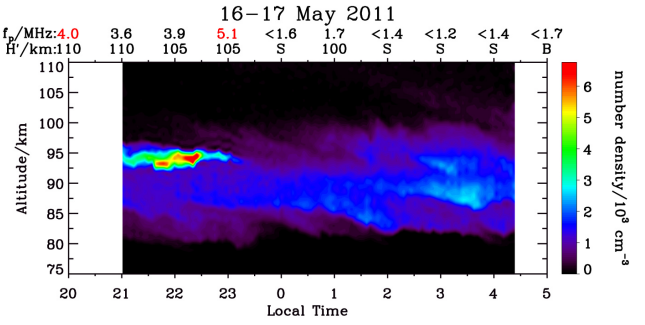

Figure 4. Na density contour plot and E_s layer parameters during the night of 16–17 May 2011. Note the temporally correlated sporadic Na and E layers occurring before midnight.

the E_s layer. As seen from Fig. 2, during the observation period of Na layers, the E_s layers appeared with f_p of 5.1 and 4.3 MHz ($N_e = 3.2 \times 10^5$ and 2.3×10^5 cm^{-3}) at 22:00 and 23:00 LT, respectively. The E_s layers were also active within ∼ 2 h before and after the observation of Na layers. However, no Na_s layer event could be found during the entire observation of lidar.

4.1.2 Case study 2 (28–29 February 2008)

As seen in Fig. 3, during the night on 28–29 February 2008, an Na_s layer occurred near 95 km at 22:23 LT. It grew very rapidly and reached its maximum peak number density of near 21 600 cm^{-3} near 91.8 km at 22:40 LT. Then this extremely strong Na_s layer gradually decayed and finished at 01:34 LT. The layer was morphologically similar to Kelvin–Helmholtz billows (Kane et al., 2001), and it was the second strongest Na_s layer during all 95 nights of observations. However, no corresponding E_s behavior occurred around this time. In fact, the E region ionosphere was notably calm throughout the entire night, despite the appearance of this impressively strong Na_s layer. By the way, the symbol "S" of virtual height means the occurrence of interference in ionosphere; no ionosonde echo by the E_s layer can be received. In this situation, the corresponding f_p recorded by the ionosonde represents the lowest frequency of undisturbed ionosonde echoes. Consequently, the real plasma frequency of the E_s layer, which may exist, would only be less than the value of recorded f_p.

4.1.3 Case study 3 (16–17 May 2011)

The above two cases represent the singly appearing E_s and Na_s layers. Now we show a case of temporally correlated sporadic Na and E layers on the night of 16–17 May 2011. As seen in Fig. 4, a Na_s layer was already growing near ∼ 94.1 km when the observation began at 21:01 LT. It reached its maximum peak density of ∼ 7510 cm^{-3} near 93.9 km at 22:24 LT. The Na_s layer lasted

Table 3. The statistical correlation of Na_s and E_s layers over Qingdao.

Correlation of Na_s and E_s layers	Number of events
Total number of Na_s layers	53
Na_s layers without E_s layers	27 (51 %)
Na_s layers with E_s layers	
Total number	26 (49 %)
$-2\,h \le \Delta t < -1\,h$	7
$-1\,h \le \Delta t \le 1\,h$	17 (32 %)
$1\,h < \Delta t \le 2\,h$	2

for more than 2 h and finished at 23:14 LT. With respect to the f_p, it was more than 3.5 MHz from 20:00 to 23:00 LT. And the E_s event occurred at 23:00 LT with f_p of 5.1 MHz. Then the f_p suddenly fell below 1.6 MHz at 00:00 LT and never exceeded 1.7 MHz until dawn. Generally speaking, the period of this Na_s layer covered the occurrence of the E_s layer. And the time difference between maximum Na_s layer peak density and maximum f_p was 36 min. By the way, the symbol "B" (at 05:00 LT) of virtual height means the occurrence of absorption in the ionosphere.

4.2 Statistics study

The correlation of Na_s and E_s layers is normally confirmed by the difference of their occurrence time. Here we use Δt to represent the difference of occurrence time for a Na_s layer and an E_s layer. The confirmation of a pair of correlated Na_s and E_s layers requires Δt to be within ± 2 h (Alpers et al., 1994; Hansen and von Zahn, 1990). Table 3 lists the detailed correlation of Na_s and E_s layers at our site. The Δt with a positive value means that an E_s layer lags behind its corresponding Na_s layer, while the Δt with a negative value means that an E_s layer occurs before its corresponding Na_s layer.

As seen in Table 3, among a total of 53 Na_s layer events, 26 (49 %) events possessed correlation with E_s layers. Furthermore, 17 (32 %) Na_s layers occurred within ± 1 h of their corresponding E_s layers. Figure 5 shows the height and peak number density distribution of all Na_s layer events. The Na_s layers occurring without E_s layers are drawn in hollow circles, and the others are drawn in solid symbols. Different solid symbols represent different value ranges of Δt. For further details, please see the figure annotation. As seen in Fig. 5, Na_s layers correlated with E_s layers generally exhibit higher altitudes. In addition, with respect to Na_s layers above 92 km, the stronger parts with peak densities great than 1×10^4 cm^{-3} are all correlated with E_s layers.

5 E_s layer occurrence probabilities around Na layers

As we know, a reliable correlation between one Na_s layer and one E_s layer can only be established based on data with high enough temporal and spatial resolutions, such as the Na_s and E_s layer pair evolving with the same track obtained by lidar and incoherent scatter radar on 16 January 1989 at Arecibo (Beatty et al., 1989). However, considering the comparably low resolutions (1 h and ± 5 km) of E_s layer data obtained by our ionosonde, the claim of correlation between Na_s and E_s layers obtained above is crude. The extent of correlation between Na_s and E_s layers is still a mystery. Therefore, we will further study the correlation between Na_s and E_s layers by surveying E_s layer occurrence probabilities in three different time intervals around a Na_s layer. As seen in Fig. 6a, the first time interval is the period within 2 h before the Na_s layer initiates. The second time interval matches the occurrence duration of the Na_s layers. The third time interval is the period within 2 h after the Na_s layer dissipates. Noticing that the ionosonde operates every hour on the hour, it operates twice in both the first interval and the third interval. Whereas, the number of ionosonde scans in the second interval is not fixed and could be several or none (Fig. 6b). As seen in Fig. 6c, a Na_s layer could already exist when the lidar observation begins. In this case, the real beginning time point of a Na_s layer has not been caught. Hence its first interval is not knowable and available. Similarly, the third interval could be unavailable if a Na_s layer still exists when lidar observation stops (Fig. 6d).

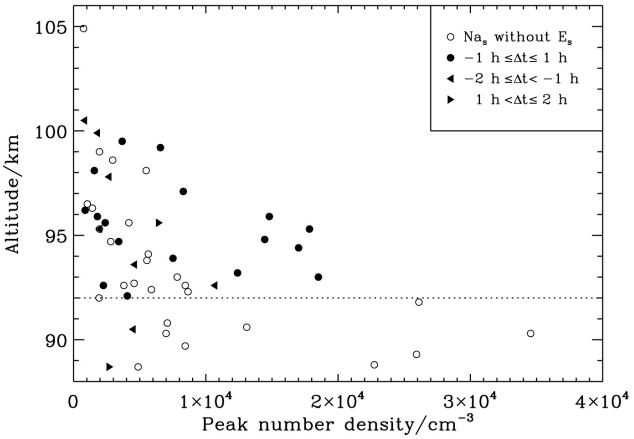

Figure 5. Altitude and peak number density of all Na_s layers. Δt represents the difference of occurrence time for Na_s and E_s layers. Positive value of Δt means that a Na_s layer occurs before an E_s layer. While a negative value of Δt means that a Na_s layer lags behind an E_s layer.

Using these intervals to analyze all 53 Na_s layers, we have obtained the total number of ionosonde operation times for each of the three time intervals. As seen in Table 4, the ionosonde made 70, 86, and 88 scans in the first, second, and third intervals, respectively. By calculation, occurrence probabilities of E_s layers in the same three time intervals are 19 % (13/70), 22 % (19/86), and 18 % (16/88). Very importantly, the advantage of introducing these three probabilities is their mathematical comparability with the average

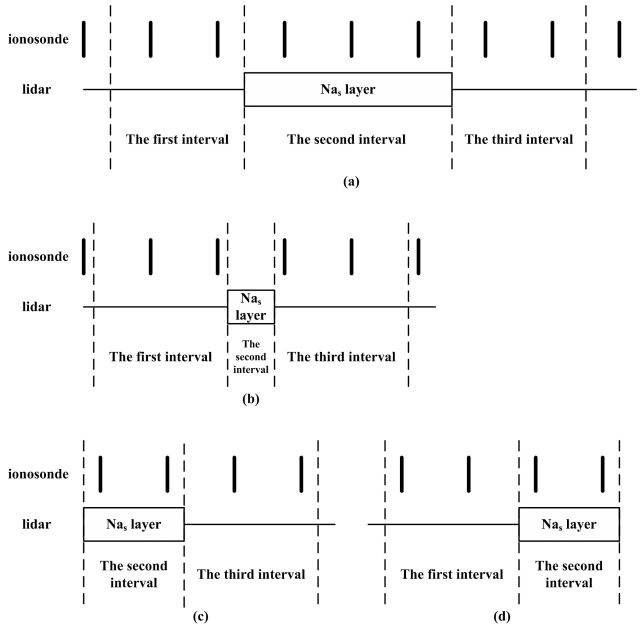

Figure 6. The definition of three time intervals around the Na_s layer.

nocturnal E_s layer occurrence ratio. Obviously, if the occurrence of Na_s and E_s layers is mutually independent, the values of E_s layer occurrence probabilities in three time intervals should all tend to the average E_s layer occurrence ratio. As mentioned above, the average occurrence ratio of E_s layers (f_p reaching 4 MHz) during the night over Qingdao is 21 %. Therefore, the fact that E_s layer occurrence probabilities in three time intervals (19, 22, and 18 %) are very close to the E_s layer occurrence ratio at night (21 %) should reveal the general independence between Na_s and E_s layer events over Qingdao. In other words, it seems the fact that the coincidence probabilities between E_s and Na_s layers are the same as their incidence probabilities is a pretty strong argument that any coincidence of E_s and Na_s layers is exactly that, a coincidence.

Guided by Fig. 5, we have further surveyed E_s layer occurrence probabilities around different samples of Na_s layers in Table 4. With respect to the Na_s layers above 92 km, E_s layer occurrence probabilities in three intervals are 22 % (12/54), 26 % (19/74), and 22 % (15/68), respectively. And E_s layer occurrence probabilities around Na_s layers with peak density above 10^4 cm^{-3} and altitude above 92 km are 67 % (10/15), 88 % (7/8), and 40 % (4/10). These values are much higher than the average occurrence ratio of E_s layers at night (21 %). Thus it might suggest that only those strong Na_s layers above the peak altitude of the main Na layer have a correlation with E_s layers. Nevertheless the number of such samples may be insufficient.

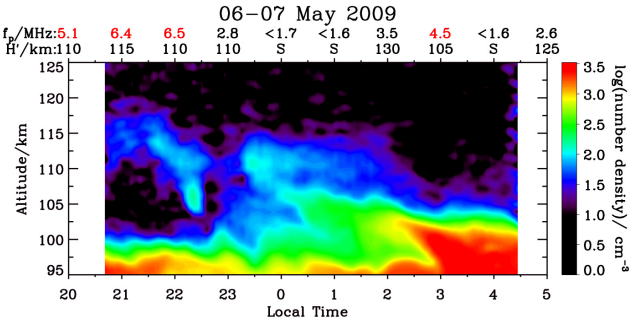

Figure 7. Na density contour plot and E_s layer parameters during the night of 6–7 May 2009, which displayed a high-altitude Na_s layer above 105 km. Notice the correlation between the Na_s and E_s layer events on this night seemed good.

6 Characteristics of high-altitude sporadic Na layers

Considering the fact that the detection ability of lidar decreases with increasing altitude, we have decreased the temporal resolution of Na data to 15 min by integrating several raw photon count profiles, in order to ensure a good data quality. Referring to our previous work, the high-altitude Na_s layers are defined to match three criteria: (1) the altitude is above 105 km. (2) The peak density is greater than 50 cm^{-3}, which is five times of corresponding detection threshold (10 cm^{-3}) at 110 km. (3) The layer lasts for at least 45 min (three consecutive profiles).

6.1 Case studies

6.1.1 Case study 1 (6–7 May 2009)

In our previous work, we found a phenomenon that the high-altitude sporadic Na layers appeared on the same night (18–19 May) in two different years (2001 and 2006) at Wuhan (Ma and Yi, 2010). Interestingly, this reappearance phenomenon of high-altitude Na_s layers also occurred at Qingdao.

Figure 7 displays a Na density contour plot during the night of 6–7 May 2009. A high-altitude sporadic Na_s layer was distinguished around 115 km at 21:00 LT. Then it gradually descended and reached its maximum peak density of 128 cm^{-3} near 110.7 km at 23:30 LT. At the same time, its FWHM and column abundance were 4.05 km and $\sim 4 \times 10^7$ cm^{-2}, respectively. This Na_s layer existed for about 5 h and finished after 01:45 LT when it merged with the main Na layer. With respect to the E_s layer, it reached the plasma frequency of 6.4–6.5 MHz during the formation period of the Na_s layer, and then was less than 4 MHz until the Na_s layer finished. Generally speaking, the correlation between the Na_s and E_s layer events on this night seemed good.

Table 4. The statistical occurrence probability of E_s layers in three different time intervals around Na_s layers.

Sample of Na_s layers	Number of Na_s layer events	Time intervals: within 2 h before Na_s layers	during Na_s layers	within 2 h after Na_s layers
All	53	19 % (13/70)	22 % (19/86)	18 % (16/88)
above 92 km	42	22 % (12/54)	26 % (19/74)	22 % (15/68)
$> 10^4$ cm^{-3} and above 92 km	7	67 % (10/15)	88 % (7/8)	40 % (4/10)

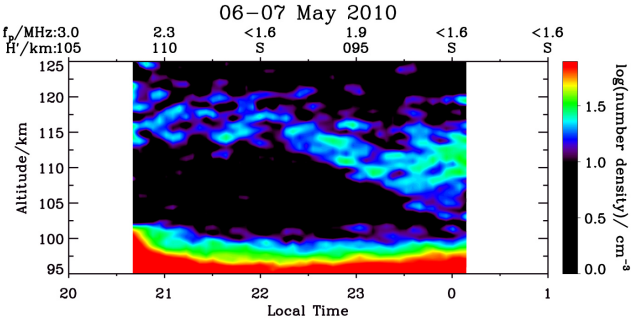

Figure 8. Na density contour plot and E_s layer parameters during the night of 6–7 May 2010, which displayed a high-altitude Na_s layer above 105 km. Notice the E_s layer did not occur during the entire observation of the Na layer.

6.1.2 Case study 2 (6–7 May 2010)

As seen in Fig. 8, the high-altitude sporadic layers reappeared 1 year later (6–7 May 2010). This Na_s layer formed at 116 km around 21:45 LT, and descended all along. It reached its maximum peak density of 71 cm^{-3} near 110.7 km at 23:45 LT. At the same time, its FWHM width and column abundance were 6.00 km and $\sim 3 \times 10^7$ cm^{-2}. This Na_s layer was still apparent when the lidar observation stopped at 00:15 LT. So it lasted for more than 165 min. However, with respect to an E_s layer, none occurred during the entire observation of the Na layer. Finally, notice both the high-altitude Na_s layers on the nights of 6–7 May in 2009 and 2010 possessed weak number density, broad layer width and long duration.

6.2 Statistics study

First of all, a total of 11 high-altitude (above 105 km) Na_s layer events have been selected from 95-night lidar data. Some characteristics of high-altitude Na_s layers over Qingdao as well as those over Wuhan are shown in Table 5. Note that the sensitivity of lidar at Qingdao is higher than that at Wuhan due to the larger telescope aperture. By comparing the results in Tables 2 and 5, it is very obvious that high-altitude Na_s layers over Qingdao possessed long duration (> 147 min) and broad layer width (4.0 km) compared with

Table 5. Statistical characteristics of high-altitude (above 105 km) Na_s layers observed at Qingdao and Wuhan, China.

Location	Wuhan (30° N)	Qingdao (36° N)
Reference	Ma and Yi (2010)	this work
Number of observed Na_s layer	12 events/178 nights	11 events/95 nights
Peak density/cm^{-3}	> 200	> 50
Average duration/min	> 197	> 147
Average width (FWHM)/km	3.4	4.0

Na_s layers below 105 km (> 96 min and 2.4 km). These characteristics accord with the observational results at Wuhan.

Figure 9 has shown the seasonal distribution of high-altitude Na_s layer events, and their intensities (peak densities) have been denoted by solid circles with different colors. The cyan bars represent the total number of observation nights in each month. As seen from Fig. 9, high-altitude Na_s layers all occurred from April to August. This indicates that there exists a strong seasonal/annual distribution of high-altitude Na_s layers. The peak densities of these high-altitude Na_s layers were very small. Among a total of 11 Na_s layer events, 9 and 4 of them had the peak densities of less than 200 and 100 cm^{-3}, respectively. For the identical peak density threshold of 200 cm^{-3}, the occurrence rates of high-altitude Na_s layers were 1/215 h^{-1} over Qingdao and 1/113 h^{-1} over Wuhan.

By a similar statistical work, E_s layer occurrence probabilities in the three time intervals around high-altitude Na_s layers are 33 % (4/12), 41 % (11/27), and 13 % (1/8), respectively. Nevertheless, it should be noticed that all high-altitude Na_s layers appeared from April to August. By calculation, the corresponding average occurrence rate of the E_s layer during the nights from April to August is 40 %. Hence, the fact that the E_s layer occurrence probabilities are less than or approximately equal to the corresponding average occurrence rate of E_s layers (40 %) might suggest little correlation between high-altitude Na_s layers and E_s layers over Qingdao. Nevertheless, we point out that the numbers of ionosonde measurements are insufficient for a good statistical study.

Figure 10 draws the seasonal variation of the nocturnal mean Na atom density in which all sporadic layers have been retained. To preferentially show the Na atom number densities with small values, the density is drawn on a logarithmic scale. In addition, the red dots under the bottom of the panel

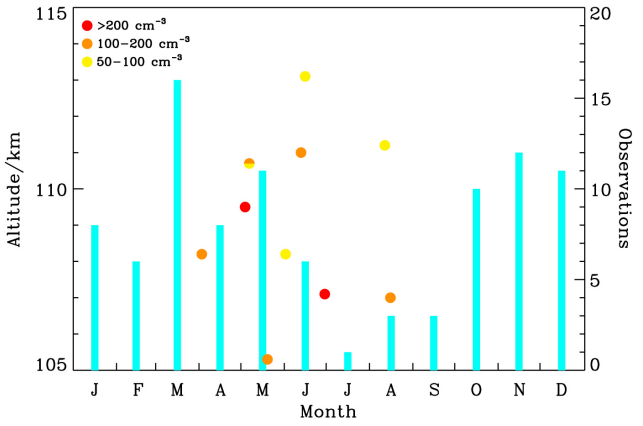

Figure 9. Seasonal distribution of peak altitudes for the high-altitude Na_s layers over Qingdao (36° N). The peak densities are denoted by the color of solid circles. Cyan bars represent the night number of the lidar measurements in each month. Note that high-altitude Na_s layers all occurred from April to August.

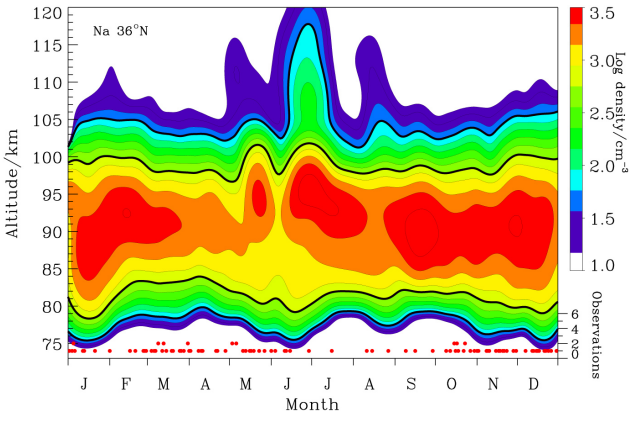

Figure 10. Na density at Qingdao (36° N) on logarithmic scales. For further explanation please see text.

together with the right-hand ordinate represent the number of observation nights on a given day. It should be pointed out that the observations from mid-June to mid-August are sparse. A detailed explanation has been given in Sect. 2.4 of Ma and Yi (2010). As seen in Fig. 10, with respect to the topside layer, there exists significant Na atom enhancement just prior to and during summer (from April to August). This feature at Qingdao (36° N) is general in agreement with several earlier observational results at different sites (18, 30, and 54° N) in the Northern Hemisphere (Höffner and Friedman, 2004; Ma and Yi, 2010).

7 Summary

We have surveyed the characteristics of sporadic Na layers based on lidar observations from December 2007 to June 2012 at Qingdao. A total of 53 Na_s layers have been selected from ∼430 h of Na number density data on 95 nights. By comparison, it is found that the occurrence rate and strength of Na_s layers over Qingdao are all close to those over Wuhan. And the average width and altitude of Na_s layers over Qingdao are close to those over Hefei. However, the strength and average altitude of Na_s layers over Qingdao are much different with those over Hachioji. Overall, the characteristics of Na_s layers over Qingdao have a general similarity with those over nearby sites, but not with those over the site at nearly the same latitude as Qingdao.

Sporadic E layers were simultaneously observed by an ionosonde standing at only ∼30 m horizontal distance from the lidar. Among a total of 53 Na_s layer events, 26 (49 %) events possessed temporal correlation with E_s layers. Furthermore, 17 (32 %) Na_s layers occurred within ±1 h of their corresponding E_s layers. However, considering the comparably low resolutions of E_s layer data obtained by our ionosonde, we are unable to conclude that there is correlation between the Na_s and E_s layers obtained above. So we have further surveyed E_s layer occurrence probabilities in three different time intervals around Na_s layers. By calculation, E_s layer occurrence probabilities in time intervals within 2 h before, during, and within 2 h after Na_s layers are 19, 22, and 18 %, respectively. The fact that E_s layer occurrence probabilities in these three time intervals are very close to the occurrence ratio of E_s layers at night (21 %) should indicate the general statistical independence between Na_s and E_s layers over Qingdao. The subset of Na_s layers with peak density above 10^4 cm^{-3} and altitude over 92 km have higher coincidence probabilities with E_s layers: 67 % for E_s occurring 2 h before Na_s, 88 % for concurrent layers, and 40 % for E_s within 2 h following Na_s. These values are much higher than the average occurrence ratio of E_s layers at night (21 %). Thus it might suggest that only those strong Na_s layers above the peak altitude of the main Na layer have correlation with E_s layers, although the number of events is still too small to reach a firm conclusion.

Na_s layers at high altitude deserve special attention. It is found that high-altitude Na_s layers over Qingdao possess long duration (> 147 min) and broad layer width (4.0 km) compared with normal ones (> 96 min and 2.4 km). These characteristics agree with our observational results at Wuhan. Similarly, the fact that E_s layer occurrence probabilities during high-altitude Na_s layers (33, 41, and 13 %) are less than or approximately equal to the corresponding occurrence rate of E_s layers (40 %) suggests insignificant correlation between this kind of Na_s layers and E_s layers. Finally, the summer topside enhancement phenomenon of Na atoms observed at Qingdao is in accord with several earlier observational results at different sites (18, 30, and 54° N) in the Northern Hemisphere.

Acknowledgements. This research is supported by National Natural Science Foundation of China through grant 41104102. The authors appreciate Shaohong He, Xiaobing Wang and Zhengzheng Ma for their technical support in collecting ionosonde and lidar data. The authors also greatly appreciate the anonymous referees for enlightening and helpful comments.

Topical Editor C. Jacobi thanks two anonymous referees for their help in evaluating this paper.

References

Alpers, M., Höffner, J., and von Zahn, U.: Sporadic Fe and E layers at polar, middle, and low latitudes, J. Geophys. Res., 99, 14971–14985, 1994.

Batista, P. P., Clemesha, B. R., and Simonich, D. M.: Horizontal structures in sporadic sodium layers at 23 degrees south, Geophys. Res. Lett., 18, 1027–1030, 1991.

Beatty, T. J., Collins, R. L., Gardner, C. S., Hostetler, C. A., Sechrist Jr., C. F., and Tepley, C. A.: Simultaneous radar and lidar observations of sporadic E and Na layers at Arecibo, Geophys. Res. Lett., 16, 1019–1022, 1989.

Clemesha, B. R.: Sporadic neutral metal layers in the mesosphere and lower thermosphere, J. Atmos. Terr. Phys, 57, 725–736, 1995.

Clemesha, B. R., Kirchhoff, V. W. J. H., Simonich, D. M., and Takahashi, H.: Evidence of an extraterrestrial source for the mesospheric sodium layer, Geophys. Res. Lett., 5, 873–876, 1978.

Clemesha, B. R., Batista, P. P., and Simonich, D. M.: An evaluation of the evidence for ion recombination as a source of sporadic neutral layers in the lower thermosphere, Adv. Space Res., 24, 547–556, 1999.

Collins, R. L., Hallinan, T. J., Smith, R. W., and Hernandez, G.: Lidar observations of a large high-altitude sporadic Na layer during active aurora, Geophys. Res. Lett., 23, 3655–3658, 1996.

Collins, S. C., Plane, J. M. C., Kelley, M. C., Wright, T. G., Soldan, P., Kane, T. J., Gerrard, A. J., Grime, B. W., Rollason, R. J., Friedman, J. S., González, S. A., Zhou, Q., Sulzer, M. P., and Tepley, C. A.: A study of the role of ion-molecule chemistry in the formation of sporadic sodium layers, J. Atmos. Sol.-Terr. Phys., 64, 845–860, 2002.

Cox, R. M. and Plane, J. M. C.: An ion-molecule mechanism for the formation of neutral sporadic Na layers, J. Geophys. Res., 103, 6349–6359, 1998.

Delgado, R., Friedman, J. S., Fentzke, J. T., Raizada, S., and Tepley, C. A.: Sporadic metal atom and ion layers and their connection to chemistry and thermal structure in the mesopause region at Arecibo, J. Atmos. Sol.-Terr. Phys., 74, 11–23, doi:10.1016/j.jastp.2011.09.004, 2012.

Dou, X., Qiu, S., Xue, X., Chen, T., and Ning, B.: Sporadic and thermospheric enhanced sodium layers observed by a lidar chain over China, J. Geophys. Res., 118, 6627–6643, 2013.

Dou, X.-K., Xue, X.-H., Chen, T.-D., Wan, W.-X., Cheng, X.-W., Li, T., Chen, C., Qiu, S., and Chen, Z.-Y.: A statistical study of sporadic sodium layer observed by Sodium lidar at Hefei (31.8° N, 117.3° E), Ann. Geophys., 27, 2247–2257, doi:10.5194/angeo-27-2247-2009, 2009.

Friedman, J. S., González, S. A., Teplay, C. A., Zhou, Q., and Sulzer, M. P.: Simultaneous atomic and ion layer enhancements observed in the mesopause region over Arecibo during the Coqui II sounding rocket campaign, Geophys. Res. Lett., 27, 449–452, 2000.

Fiorani, L., Armenante, M., Capobianco, R., Spinelli, N., and Wang, X.: Self-aligning lidar for the continuous monitoring of the atmosphere, Appl. Optics, 37, 4758–4764, 1998.

Gardner, C. S., Kane, T. J., Senft, D. C., Qian, J., and Papen, G. C.: Simultaneous observations of sporadic E, Na, Fe, and Ca^+ layers at Urbana, Illinois: Three case studies, J. Geophys. Res., 98, 16865–16873, 1993.

Gong, S. S., Yang, G. T., Wang, J. M., Cheng, X. W., Li, F. Q., and Wan, W. X.: A double sodium layer event observed over Wuhan, China by lidar, Geophys. Res. Lett., 30 , 1209–1212, doi:10.1029/2002GL016135, 2003.

Hansen, G. and von Zahn, U.: Sudden sodium layers in polar latitudes, J. Atmos. Terr. Phys., 52, 585–608, 1990.

Höffner, J. and Friedman, J. S.: The mesospheric metal layer topside: a possible connection to meteoroids, Atmos. Chem. Phys., 4, 801–808, doi:10.5194/acp-4-801-2004, 2004.

Höffner, J. and Friedman, J. S.: The mesospheric metal layer topside: examples of simultaneous metal observations, J. Atmos. Sol.-Terr. Phys., 67, 1226–1237, 2005.

Kane, T. J. and Gardner, C. S.: Structure and seasonal variability of the nighttime mesospheric Fe layer at midlatitudes, J. Geophys. Res., 98, 16875–16886, 1993.

Kane, T. J., Hostetler, C. A., and Gardner, C. S.: Horizontal and vertical structure of the major sporadic sodium layer events observed during the ALOHA-90 campaign, Geophys. Res. Lett., 18, 1365–1368, 1991.

Kane, T., Grime, B., Franke, S., Kudeki, E., Urbina, J., Kelley, M., and Collins, S.: Joint observations of sodium enhancements and field-aligned ionospheric irregularities, Geophys. Res. Lett., 28, 1375–1378, 2001.

Kwon, K. H., Senft, D. C., and Gardner, C. S.: Lidar observations of sporadic sodium layers at Mauna Kea Observatory, Hawaii, J. Geophys. Res., 93, 14199–14208, 1988.

Ma, Z. and Yi, F.: High-altitude sporadic metal atom layers observed with Na and Fe lidars at 30° N, J. Atmos. Sol.-Terr. Phys., 72, 482–491, 2010.

Nagasawa, C. and Abo, M.: Lidar observations of a lot of sporadic sodium layers in mid-latitude, Geophys. Res. Lett., 22, 263–266, 1995.

Shibata, Y., Nagasawa, C., Abo, M., Maruyama, T., Saito, S., and Nakamura, T.: Lidar observations of sporadic Fe and Na layers in the mesopause region over Equator, J. Meterol. Soc. Jpn., 84, 317–325, 2006.

von Zahn, U. and Hansen, T. L.: Sudden neutral sodium layers: A strong link to sporadic E layers, J. Atmos. Terr. Phys., 50, 93–104, 1988.

von Zahn, U., von der Gathen, P., and Hansen, G.: Forced release of sodium from upper atmosphere dust particles, Geophys. Res. Lett., 14, 76–79, 1987.

Wakai, N., Ohyama, H., and Koizumi, T.: Manual of Ionogram Scaling, 3rd Version, Radio Research Laboratory, p. 1, 1987.

Williams, B. P., Croskey, C. L., She, C. Y., Mitchell, J. D., and Goldberg, R. A.: Sporadic sodium and E layers observed during the summer 2002 MaCWAVE/MIDAS rocket campaign, Ann. Geophys., 24, 1257–1266, doi:10.5194/angeo-24-1257-2006, 2006.

Williams, B. P., Berkey, F. T., Sherman, J., and She, C. Y.: Coincident extremely large sporadic sodium and sporadic E layers ob-

served in the lower thermosphere over Colorado and Utah, Ann. Geophys., 25, 3–8, doi:10.5194/angeo-25-3-2007, 2007.

Yi, F., Zhang, S., Zeng, H., He, Y., Yue, X., Liu, J., Lv, H., and Xiong, D.: Lidar observations of sporadic Na layers over Wuhan (30.5° N, 114.4° E), Geophys. Res. Lett., 29, 1345, doi:10.1029/2001GL014353, 2002.

Yi, F., Zhang, S., Yu, C., He, Y., Yue, X., Huang, C., and Zhou, J.: Simultaneous observations of sporadic Fe and Na layers by two closely colocated resonance fluorescence lidars at Wuhan (30.5° N, 114.4° E), China, J. Geophys. Res., 112, D04303, doi:10.1029/2006JD007413, 2007.

Yuan, T., Fish, C., Sojka, J., Rice, D., Taylor, M., and Mitchell, N.: Coordinated investigation of summer time mid-latitude descending E layer (Es) perturbations using Na lidar, ionosonde, and meteor wind radar observations over Logan, Utah (41.7° N, 111.8° W), J. Geophys. Res.-Atmos., 118, 1734–1746, 2013.